Crowding Effects on *Eco*RV Kinetics and Binding

Jay R. Wenner and Victor A. Bloomfield
Department of Biochemistry, University of Minnesota, St. Paul, Minnesota 55108 USA

ABSTRACT The cytosol of the cell contains high concentrations of small and large macromolecules, but experimental data are often obtained in dilute solutions that do not reflect in vivo conditions. We have studied the crowding effect that large macromolecules have on *Eco*RV cleavage by adding high-molecular-weight Ficoll 70 to reaction solutions. Results indicate that Ficoll has surprisingly little effect on overall *Eco*RV reaction velocity because of offsetting increases in V_{max} and K_m, and stronger nonspecific binding. The changes in measured parameters can largely be attributed to the excluded volume effects on reactant activities and the slowing of protein diffusion. Covolume reduction upon binding appears to reinforce nonspecific binding strength, and k_{cat} appears to be slowed by stronger nonspecific binding, which slows product release. The data also suggest that effective Ficoll particle volume decreases as its concentration increases above a few weight percent, which may be due to Ficoll interpenetration or compression.

INTRODUCTION

The study of protein-DNA interactions in dilute solution has been a popular field of study because proteins are involved in many facets of cellular regulation and function, but comparatively little work has been devoted to investigating the dynamics of protein-DNA interactions under the condition of high volume occupancy often found in vivo. In this paper we investigate the effects of macromolecular crowding on the binding affinity and catalytic rate of the restriction enzyme *Eco*RV interacting with DNA.

In another communication (Wenner and Bloomfield, 1999), we have investigated the effects of small molecules on *Eco*RV kinetics, but living systems also function in concentrated environments of high-molecular-weight macromolecules. Muscle cells contain ~23% protein by weight, and a typical cell contains 20–30 vol % protein (Han and Herzfeld, 1993). The nucleic acid concentration in *Escherichia coli* is ~200–400 mg/ml (Record et al., 1998a), and for T4 phage heads it is ~800 mg/ml (Kellenberger et al., 1986). This compares to protein and DNA concentrations of <1%, which is common for in vitro experiments.

Zimmerman and Minton have reviewed a number of experimental systems to support the assertion that crowding promotes molecular association (Zimmerman, 1993; Zimmerman and Minton, 1993). A recent review reinforces crowding theory with examples of protein-protein, protein-DNA, and cytoskeletal interactions (Minton, 1997). Since this 1997 review, researchers have implicated molecular crowding as influential in actin polymerization and TyrR regulatory protein binding (Lindner and Ralston, 1997; Poon et al., 1997).

Received for publication 21 May 1999 and in final form 24 August 1999.
Address reprint requests to Dr. Victor A. Bloomfield, Department of Biochemistry, University of Minnesota, 1479 Gortner Avenue, St. Paul, MN 55108. Tel.: 612-625-2268; Fax: 612-625-5780; E-mail: victor.a.bloomfield-1@tc.umn.edu.

0006-3495/99/12/3234/08 $2.00

High concentrations of large macromolecules displace water, and the amount of free water in vivo is surprisingly small. Record and co-workers have found that ~0.5 g of water was bound per gram of macromolecule in the cytoplasm of *E. coli* regardless of external osmotic pressure, a figure that agreed with estimates of macromolecular hydration (see Record et al., 1998b, and references therein). Only three- to sixfold this amount was found as free water when the external solution pressure was dropped from 1.0 to 0.1 osmolal. These findings underscore two important points regarding in vivo conditions: 1) the amount of free water in the cytoplasm bears little resemblance to typical dilute solution experiments, and 2) a twofold reduction in free water volume may increase effective macromolecular concentrations or activities by several orders of magnitude (Dinnbier et al., 1988; Record et al., 1998b). Record et al. (1998a) have proposed that additional protein-DNA association resulting from macromolecular crowding may be counteracted by the uptake of K^+ as the external solution pressures rise.

Thermodynamic equations describing ideal solutions can be modified to treat excluded volume by replacing concentration (c) with activity (a) and stipulating $a = yc$, where y is an activity coefficient. The nonideal components can then be collected into a factor Γ, the product and quotient of activity coefficients, which describes the nonideal perturbations of binding or rate parameters (K_o) measured in dilute solution (Zimmerman and Minton, 1993).

To a first-order approximation, nonideal interactions are the consequence of a background agent occupying volume. Crowded solutions will favor association because the volume available to a reactant is reduced, thereby increasing the effective reactant concentration. Crowded solutions also favor a reduction in reactant covolume, which occurs when reactants associate. By these arguments, excluded volume increasingly favors monomer association to form dimers, trimers, tetramers, and polymers (Minton, 1981). At fractional occupancies found in vivo, the nonideal effects of excluded volume are expected to raise association constants

by up to several orders of magnitude relative to dilute solution values (Zimmerman and Minton, 1993).

More exact approximations of activity coefficients show that number density and molecular shape also influence excluded volume. For example, spherical conformations are favored over elongated conformations, and side-by-side association is preferred over end-to-end binding (Minton, 1981). These findings can be distilled to the basic concept that crowding favors processes that minimize surface area for a constant volume.

Nonideal interactions may also include other factors such as hydration, hydrodynamic, and electrostatic forces (Zimmerman and Minton, 1993). Our use of Ficoll 70, a nonionic, high-molecular-weight cosolvent, emphasizes excluded volume and solution viscosity effects while minimizing changes in solution dielectric and water activity. We shall use related work (Wenner and Bloomfield, 1999) on osmotic pressure to account for small changes due to hydration effects and will be concerned primarily with the response of *Eco*RV cleavage and binding to excluded volume (steric effects) and viscosity (hydrodynamic effects).

Our system contains a low concentration of *Eco*RV (a protein probe) and specific DNA (the target site) within a high concentration of Ficoll (a crowding agent or background solute) (Fig. 1 *A*). The fractional volume occupancy (ϕ) refers to the total volume occupied by all solutes, of which the crowding agent comprises the vast majority. Excluded volume is the volume from which a macromolecule is excluded, which occurs because two macromolecules cannot occupy the same space at the same time (Zimmerman, 1993). Excluded volume is synonymous with covolume, which is determined by the distance between the center of mass of a reference particle in relation to the other macromolecules in solution upon closest approach (Fig. 1 *B*). Crowding refers to excluded volume effects, with an emphasis on in vivo conditions.

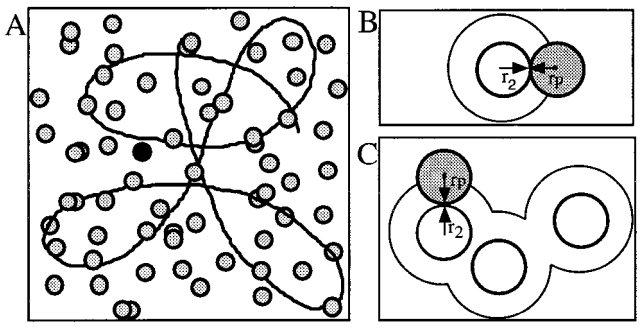

FIGURE 1 (*A*) An illustration of the *Eco*RV reaction system shows *Eco*RV (*dark shaded circle*), pBR322 (*curved line*), and Ficoll 70 (*light shaded circle*) scaled to the approximate size for a radius of hydration (R_H) for *Eco*RV (5.0 nM), Ficoll 70 (5.5 nM), and pBR322 (74 nm). The pBR322 R_H of 74 nm has been determined from $R_H = 0.665R_G$, where the radius of gyration, $R_G = (AL/6)^{0.5}$, has been determined to be 112 nm from a persistence length (A) of 50 nm, and a contour length (L) of (4361 bp)(0.34 nm/bp) = 1500 nm. Ficoll 70 has been represented as uniformly sized, although the reaction system contains a distribution of Ficoll molecular weights (Fig. 2). (*B*) The thin line of radius $2r_2 = r_p + r_2$ represents the covolume between an equally sized probe of radius r_p (*dark shaded circle with depicted center of mass*) and a background agent of radius r_2 in dilute solution. (*C*) The contoured thin line represents the covolume between an equally sized probe and a background agent in more concentrated solutions where covolumes overlap (Tanford, 1961).

For dilute solutions of spherical molecules, the covolume (u) is defined by a sphere, the radius of which is obtained from the sum of the probe (p) and background solute (2) radii (Zimmerman and Minton, 1993),

$$u = \tfrac{4}{3}\pi(r_p + r_2)^3, \tag{1}$$

or for equally sized probe and solute (Tanford, 1961),

$$u = \tfrac{32}{3}\pi(r_2)^3. \tag{2}$$

From Eq. 2, the second viral coefficient can be obtained (Tanford, 1961), although in solutions of appreciable concentration, covolumes overlap (Fig. 1 *C*), and higher order viral coefficients should be used to approximate excluded volume. The geometric series

$$\frac{pV}{RT} = 1 + \sum_{n=0}^{\infty}(n^2 + 3n)u^n \tag{3}$$

closely estimates viral coefficients ($n = 1, 2, 3, \ldots$) to the seventh term (Carnahan and Starling, 1969). Equation 3 can equivalently be expressed in the more useful form

$$\frac{\pi\bar{M}_N}{C_2RT} = \frac{(1 + u + u^2 - u^3)}{(1 - u)^3}, \tag{4}$$

where π represents the osmotic pressure, $\bar{M}_N$ is the number average molecular weight, and C_2 is the molar concentration of background agent. Equation 4 or equivalent expressions based on the colligative properties of Eq. 3 have been used to successfully fit osmotic pressure, sedimentation equilibrium, and light scattering data from concentrated solutions of hemoglobin and bovine serum albumin (see Minton, 1983, and references therein).

The widely accepted model by which DNA binding proteins find their specific target is one in which they diffuse in 3D space until nonspecific DNA is bound, and then slide in a 1D search until the specific site is encountered (Riggs et al., 1970). During sliding, dissociation can occur with a reinitiation of the 3D search process. A significant body of theoretical work on this model has been presented by Berg and collaborators (Berg and Blomberg, 1976, 1977, 1978; Berg and Ehrenberg, 1982; Berg et al., 1981). The 1D sliding mechanism has been firmly established by experimental evidence for a number of proteins, including, in part, repressors, transcription factors, nucleases, and a number of endonucleases: *Bam*HI, *Bss*HII, *Hind*III, *Eco*RI, and *Eco*RV (see Jeltsch and Pingoud, 1998, and references therein).

Many crowding studies have determined association constants, but our aim is to investigate the effects of high-molecular-weight solutes on both the binding affinity and catalytic rate of *Eco*RV to DNA. Crowding through Ficoll

addition is expected to increase nonspecific binding or lower $K_{d,ns}$, where the nonspecific dissociation constant $K_{d,ns}$ is a determinant in specific site location and product inhibition. Crowding should also raise the maximum velocity V_{max}, because of an increase in enzyme activity, but the effect of Ficoll on the rate constants that define V_{max} and the Michaelis constant K_m is less certain. Minton (1983) has proposed that crowding increases association constants with little or no effect on dissociation constants, although the large size of Ficoll will increase solution viscosity, and the results of previous work with small cosolvents show that increasing viscosity raises K_m. The net result of Ficoll addition (in simulating in vivo crowding) is the sum of several opposing effects and, therefore, very difficult to predict. A traditional view may discount excluded volume effects and assume that viscous solutions would slow cleavage reactions. Excluded volume proponents may conversely predict that reaction rates will increase because higher effective reactant concentrations will overcome slowed diffusion.

To test the effects of crowding, we measured *Eco*RV reaction kinetics in solutions of Ficoll 70. We found that Ficoll addition has remarkably little effect on *Eco*RV solution activity because of offsetting changes in V_{max}, K_m, and $K_{d,ns}$. These changes agree with those expected from viscosity and excluded volume effects.

MATERIALS AND METHODS

The methods used to measure *Eco*RV cleavage kinetics, and solution density, osmometry, and viscosity have been described elsewhere (Wenner, 1999; Wenner and Bloomfield, 1999) for small cosolvents. The basic protocol is to start reactions by adding *Eco*RV to a solution of DNA and cofactor at 20.0°C. Aliquots of the reaction are combined with EDTA, which chelates the Mg^{2+} cofactor and stops the reaction. Substrate and products are then separated on agarose gels, stained with SYBR Green I, digitally scanned, and quantified for kinetic analysis. DynaFit software (http://www.biokin.com/dynafit/index.shtml) (Kuzmic, 1996) was used to globally fit an integrated rate equation to data from eight reactions consisting of duplicate experiments at four concentrations: 2.5, 1.5, 0.75, and 0.4 nM DNA.

Ficoll 70

Ficoll 70 was purchased from Pharmacia Biotechnology and used without further purification. A 45% (g/dl) stock solution (density = 1.1451 g/ml) was prepared in 1 mM HEPES (pH 7.5) and 0.01 mM EDTA. Density was measured by weighing the contents of a 50-ml volumetric flask on a Mettler AE204 analytical balance. The properties of the Ficoll solutions are given in Table 1, and its size distribution is shown in Fig. 2.

TABLE 1 Physical parameters of Ficoll in buffer solutions

Solute	Solute (%)	Viscosity (cP)	Density (g/ml)	π (mmol/kg)
Buffer*	0	1.036 ± 0.009	1.007137	248 ± 2
Ficoll 70	5	1.82 ± 0.01	1.024323	293 ± 2
Ficoll 70	10	3.14 ± 0.01	1.041193	316 ± 2
Ficoll 70	20	9.95 ± 0.01	1.075716	389 ± 2

*Buffer composition is as listed in Fig. 3 legend.

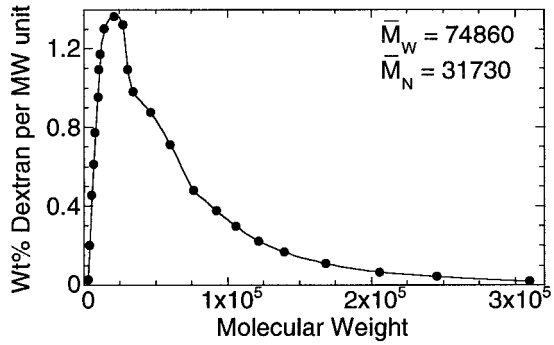

FIGURE 2 Molecular weight distribution for Ficoll 70 obtained by gel filtration with indicated weight-averaged ($\bar{M}_w$) and number-averaged ($\bar{M}_N$) molecular weight. The line fit was added by data interpolation. Original data are from Pharmacia Biotechnology.

Light scattering

Light scattering experiments were performed as previously described (Arscott et al., 1995), with a Lexel argon-ion laser operating at 488 nm, with a power output of 102 mW. Scattering from a Ficoll 70 solution (20°C) was detected by the photomultiplier tube at 90° and processed by a BI-900AT digital correlator (Brookhaven Instruments).

RESULTS

Reaction mechanism

We used a generalized Michaelis-Menten mechanism including nonspecific binding to substrate S or product P, which can be more succinctly written as a single nonspecific binding of enzyme to S_i, where $[S_i] = [S] + [P]$ represents the initial concentration of DNA substrate (or total concentration of binding sites):

$$E + S \underset{k_{r1}}{\overset{k_{f1}}{\rightleftharpoons}} ES^*$$

$$ES^* \xrightarrow{k_{cat}} E + P$$

$$E + S_i \overset{K_{d,ns}}{\rightleftharpoons} ES_i.$$

Data fitting

The k_{f1} values in fits of 5%, 10%, and 20% (g/dl) data were reduced by a factor D_t/D_o obtained from Ficoll self-diffusion studies (see Eq. 11 in the Discussion) to account for the large effects of Ficoll on solution viscosity. When a constant value of $k_{f1} = 7.2\ nM^{-1}\ min^{-1}$ ($1.2 \times 10^8\ M^{-1}\ s^{-1}$) (Erskine et al., 1997) was used, the fitted value of k_{r1} was reduced to near zero, but final V_{max}, K_m, and $K_{d,ns}$ values were within the error of those obtained when k_{f1} was varied. Slowing k_{f1} more accurately represents solution dynamics and provides slightly more accurate fits because the fitted

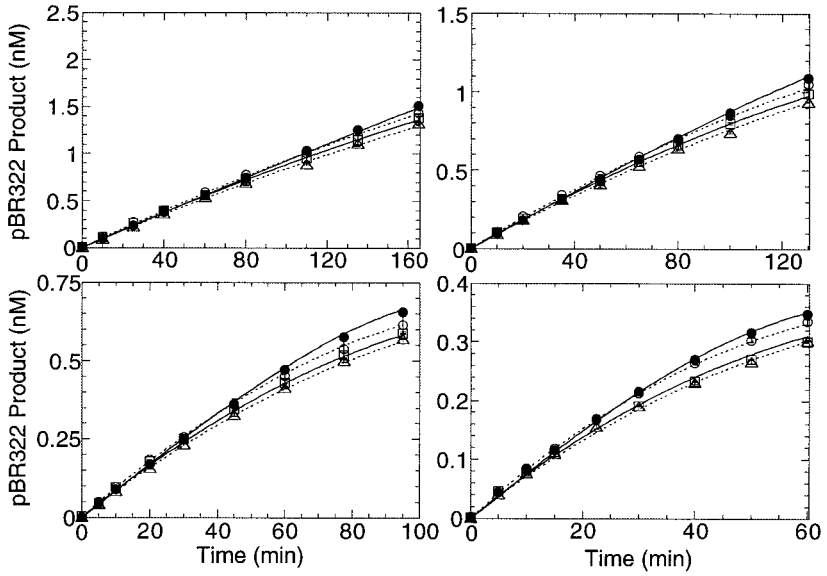

FIGURE 3 *Eco*RV cleavage of linear pBR322 at 2.5, 1.5, 0.75, and 0.40 nM pBR322 DNA chains in (●) no added Ficoll 70, (○) 5% (g/dl) Ficoll 70, (□) 10% Ficoll 70, and (△) 20% Ficoll 70. All buffers contained 50 mM HEPES (pH 7.5), 10 mM $MgCl_2$, 100 mM NaCl, 10 mM β-mercaptoethanol, and 100 μg/ml bovine serum albumin. The data from four DNA concentrations have been simultaneously fit (a global fit) to the Michaelis-Menten mechanism, including nonspecific binding to substrate and product. See Table 2 for fit parameters. Bars representing standard error are often smaller than the data symbols.

values of k_{cat} in $K_m = (k_{cat} + k_{r1})/k_{f1}$ are appropriately independent of k_{r1} at k_{r1} values above zero.

Reactions in Ficoll 70

Fig. 3 and Table 2 compare *Eco*RV cleavage in 5%, 10%, and 20% Ficoll to cleavage without a crowding agent. A 5% Ficoll solution represents the approximate volume occupancy found in vivo ($\phi \approx 0.3$) and a 1.8-fold increase in solution viscosity compared to buffer (Table 1). These conditions are expected to significantly change kinetic parameters, yet reaction velocities nearly matched those without Ficoll. A closer examination of the data suggests that the 5% Ficoll may have accelerated the velocity during the first half of cleavage while slowing the final rates, although the difference between initial rates is within the standard error of the data.

Perhaps more surprising are the similar reaction velocities in 10% and 20% Ficoll compared to buffer. These solutions have near-gel qualities because Ficoll increases solution viscosity up to an order of magnitude and occupies a large volume fraction; yet initial reaction rates matched those without Ficoll, and the cleavage velocities diverged only modestly at the most dilute substrate concentrations or as substrate was depleted by cleavage.

TABLE 2 Kinetic parameters in Ficoll 70 solutions at pH 7.5

% Ficoll (g/dl)	Mg^{2+} (mM)	V_{max} (pM/min)	K_m (nM)	$K_{d,ns}$ (μM)
0	10	10.4 ± 0.1	0.083 ± 0.004	6 ± 1
5	10	14.0 ± 0.7	0.14 ± 0.01	1.4 ± 0.2
10	10	15 ± 1	0.19 ± 0.02	1.5 ± 0.2
20	10	15 ± 1	0.19 ± 0.03	1.4 ± 0.2
0	5	10.6 ± 0.3	0.051 ± 0.006	2.2 ± 0.6
10	5	15.7 ± 0.8	0.12 ± 0.02	0.9 ± 0.1

Fits of reaction data show distinct differences in kinetic parameters between solutions with and without Ficoll (Table 2). Solutions spanning the 0–20% Ficoll range show a 44% increase in V_{max}, a doubling of K_m, and a fourfold reduction in $K_{d,ns}$. The nearly constant reaction velocities result from increases in V_{max}, which are counteracted by higher K_m and lower $K_{d,ns}$. The increase in V_{max} and decrease in $K_{d,ns}$ agree with those expected from excluded volume effects, and the increase in K_m is consistent with increased viscosity, which slows k_{f1} more than $k_{cat} + k_{r1}$.

Excluded volume and fractional occupancy

Fig. 4 shows covolume determinations based on Eq. 4, measurements of osmotic pressure, the weight-averaged molecular weight of Ficoll (Fig. 2), and the assumption that Ficoll is a sphere of radius 5.5 nm, as shown by dynamic light scattering measurements. In addition to the 5%, 10%, and 20% solutions, osmotic pressure has been measured at 2.5% Ficoll, although kinetic data have not been obtained at this concentration.

The covolume determination at 2.5% Ficoll via Eq. 4 agrees with that from Eq. 1, which assumes no covolume overlap. As Ficoll concentrations increase from 2.5% to 10%, the covolume values decrease and approach the fractional occupancy figures obtained from $\phi = nv$, where n is the number density and v is the Ficoll volume. The decrease in covolume values and $\phi > u$ at concentrations above 10% suggest that Ficoll particle volume may decrease with solution concentration.

Excluded volume effect on Mg^{2+} concentration

Excluded volume may increase Mg^{2+} concentration and V_{max} rates if *Eco*RV is not saturated at 10 mM Mg^{2+}. *Eco*RV saturates at 1 mM Mg in 50 mM Tris buffer (Taylor

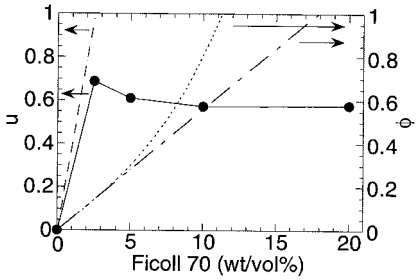

FIGURE 4 Excluded volume (u) and fractional occupancy (ϕ) values in Ficoll solutions. Excluded volume (●) has been obtained from the difference between measured values of osmotic pressure (π) in Ficoll and buffer solutions, $\bar{M}_N = 74860$, and Eq. 4. Error bars from π measurements are smaller than the data points. A line has been added to guide the eye. The medium dashed line (– – –) represents the excluded volume, with a Ficoll radius of 5.5 nm obtained from dynamic light scattering and Eq. 2. The alternating dashed line (– - –) represents the fractional occupancy calculated from $\phi = nv$, where n is the number density and v is the Ficoll volume for a sphere of radius 5.5 nm. The small dashed line (- - -) represents a third-degree polynomial fit to the fractional occupancy ϕ obtained from measured values of solution viscosity (Table 2) and the Einstein relation ($\eta/\eta_o = 1 + 2.5\phi$) (Schultz and Solomon, 1961). Arrows link plots to the appropriate axis.

and Halford, 1989), but Mg^{2+} dependence has not been tested in HEPES buffer. We measured cleavage with and without 10% Ficoll in 5 mM Mg^{2+} and found that V_{max} values were equivalent to those at 10 mM Mg^{2+}; $K_{d,ns}$ and K_m dropped as expected from ionic strength effects (Table 1). We conclude that apparent Mg^{2+} (or ionic strength) increases due to excluded volume effects do not increase V_{max} in the crowding experiments at 10 mM Mg^{2+}.

DISCUSSION

Qualitative interpretation of data

*Eco*RV cleavage in Ficoll is remarkable in that high volume occupancy and solution viscosity do not markedly change reaction velocities. In fact, the initial data assessment without the knowledge of fit parameters led to the incorrect conclusion that Ficoll has little effect on *Eco*RV dynamics. The kinetic parameters provide a more accurate assessment in that nearly uniform reaction velocities result from offsetting changes in V_{max}, K_m, and $K_{d,ns}$.

Changes in reaction parameters qualitatively agree with shifts expected from excluded volume and viscosity effects. The V_{max} and $K_{d,ns}$ parameters move in the direction predicted by concentration increases due to excluded volume effects. K_m should decrease because of excluded volume, although increases in solution viscosity may raise K_m by slowing k_{f1}. Because k_{r1} (in K_m) represents dissociation and the rate-limiting step in k_{cat} is product dissociation (Erskine et al., 1997), the numerator of K_m should be relatively immune to solution viscosity. Note that high viscosities may promote rebinding of product, but this process represents inhibition through nonspecific binding as compared to inhibition through slowed k_{r1} or product dissociation. The effects of water activity on reaction parameters should be minimal, because Ficoll changes osmotic pressure only slightly (Table 2) compared to molar concentrations of small solutes studied previously.

Quantitative interpretation of data

Quantitative evaluation of data is difficult, because Ficoll cannot be effectively modeled as a hard sphere. This assessment stems from an unreasonably large fractional occupancy value of 1.12 in 20% solution and a decrease in covolume at concentrations above 2.5% Ficoll (Fig. 4). While $\phi > 1$ is obviously not possible, values above $\phi = 0.6$ are questionable because random close packing of spheres occurs at $\phi \approx 0.6$ (Hou et al., 1990). Ficoll fractional occupancy values have been determined from $\phi = nv$, where the number density has been calculated from a weight-averaged molecular weight supplied by the manufacturer (Fig. 2), and the volume has been obtained from a weight-averaged radius determined by dynamic light scattering. At Ficoll concentrations less than 5%, ϕ values obtained from light scattering agree closely with those derived from viscosity measurements via the Einstein relation $\eta/\eta_o = 1 + 2.5\phi$ (Schultz and Solomon, 1961). Because viscosity-derived ϕ values are independent of radius and molecular weight determinations, the radius and the molecular weight determinations appear to be valid.

At concentrations of a few percent Ficoll, the covolume per added Ficoll particle will decrease because of covolume overlap, but total covolume should rise if Ficoll behaves like a rigid sphere. Fig. 4 shows that covolume increases rapidly to a maximum near 2.5% Ficoll and then decreases to a constant level of ~0.6, the value for closely packed spheres. The drop in covolume at concentrations above 2.5% Ficoll appears to result from both covolume overlap and interpenetration and/or compression of the highly branched Ficoll particle. The values of covolume and fractional occupancy appear to merge at concentrations above 10% because of close packing, and Ficoll addition to 10% solutions results in a decreased volume per particle to maintain a fixed total covolume near 0.6, the random close packing value.

To quantitatively analyze the kinetic parameters in Ficoll, we have removed the effects of water activity (which has a minor influence) and solution viscosity (which affects K_m) by using the results of small cosolvent studies (Wenner, 1999; Wenner and Bloomfield, 1999). We have then calculated apparent kinetic parameters based on the excluded volume determinations presented in Fig. 4. This approach assumes that excluded volume will change kinetic parameters by increasing reactant activities through a reduction in available volume. By comparing measured and calculated parameters, we then assess other factors that may influence measured parameters.

Excluded volume will reduce the volume available ($1 - u$) to reactants and increase reactant activity by

$$a_i = \frac{C_i}{1-u}, \tag{5}$$

where i = protein (p), DNA (d), or complex (c). For the equilibrium p + d ⇔ c, the dissociation constant is given by

$$K_d = \frac{a_p a_d}{a_c} \tag{6}$$

and the apparent value by

$$K_{d(app)} = \frac{C_p C_d}{C_c}. \tag{7}$$

Combining Eqs. 5, 6, and 7 gives

$$K_{d(app)} = K_d(1-u). \tag{8}$$

$K_{d(app)}$ represents the calculated values of $K_{d,ns(app)}$ and $K_{m(app)}$ in Ficoll solutions, K_d represents the measured values of $K_{d,ns}$ and K_m in dilute solution, and u is the excluded volume from Fig. 4. $V_{max(app)}$ values will increase by a factor $(1-u)^{-1}$ due to excluded volume effects on enzyme concentration:

$$\frac{V_{max(app)}}{V_{max}} = \frac{a_p}{c_p} \tag{9}$$

$$V_{max(app)} = \frac{V_{max}}{1-u}. \tag{10}$$

$V_{max(app)}$ represents the calculated values in crowded solution, and V_{max} is the measured value in dilute solution, similar to $K_{d(app)}$ above.

$K_{d,ns}$ interpretation

Most of the decrease in the calculated value of $K_{d,ns(app)}$ results from excluded volume effects, although the estimate also includes a small modification obtained from data with small cosolvents, $K_{d,ns} = [-174 + 180a_w]$ nM, to account for changes in water activity (a_w) that occur because of Ficoll addition. Fig. 5 shows that the measured values of $K_{d,ns(app)}$ are lower than the calculated values. The difference is likely due to a reduction in reactant covolume that occurs upon binding. Both an increase in effective reactant concentration due to Ficoll volume occupancy and a reduction in covolume due to binding will favor nonspecific binding in crowded environments (Minton, 1983; Poon et al., 1997). It is difficult to quantify this effect from reactant-Ficoll covolumes because the DNA substrate has a worm-like chain configuration, and the radius of the background agent appears to change with concentration.

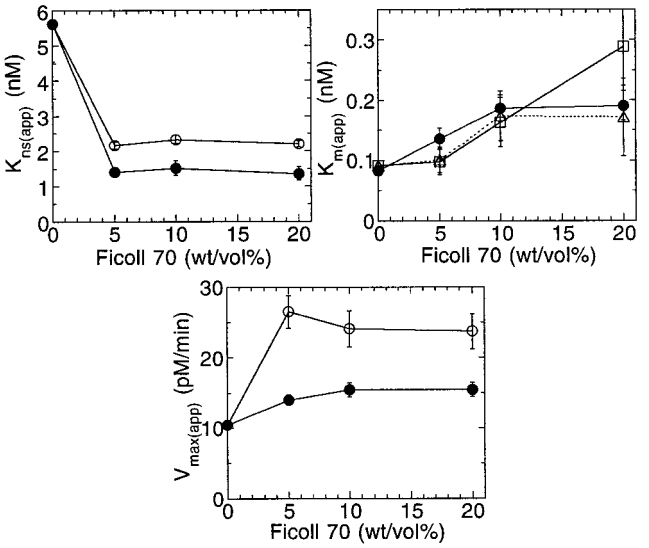

FIGURE 5 Comparison of calculated (○, □, △) and measured (●) apparent kinetic parameters in Ficoll 70 solutions. $K_{d,ns(app)}$ and $V_{max(app)}$ calculations are based on excluded volume effects and include compensation for changes in water activity. The $K_{m(app)}$ calculation also accounts for changes in diffusion by use of a stretched exponential equation (□) or the Einstein relation (△) as described in the text.

K_m interpretation

The increase in calculated $K_{m(app)}$ results from more viscous solutions, overwhelming the excluded volume and water activity effects. The viscosity dependence of K_m is the consequence of slowed diffusion, but an increase in solution viscosity due to Ficoll addition does not reduce *Eco*RV diffusion by a factor of η/η_o, reflecting the ratio of macroscopic viscosity with and without Ficoll. *Eco*RV and Ficoll are approximately the same size ($R_{H(EcoRV)} \approx 5.0$ nm (Winkler et al., 1993), $R_{H(Ficoll)} \approx 5.5$ nm), and tracer diffusion studies have shown that the η/η_o factor underestimates Ficoll 70 self-diffusion. Self-diffusion rates measured in solutions of Ficoll 70 and 400 have been fit by the stretched exponential scaling equation (Hou et al., 1990)

$$D_t/D_o = \exp(-0.035c^{0.635}R_H^{0.16}), \tag{11}$$

where c is the Ficoll concentration in g/L and R_H is the approximate tracer (*Eco*RV) radius in nm.

The η/η_o factor assumes ideal Newtonian fluid dynamics, where background particle size is insignificant compared to the diffusing species. When background particle size is large compared to the probe, diffusion occurs in the void volume between (relatively stationary) particles, and a reduction in search dimensionality corresponds to an increase in diffusion rate. Hou et al. (1990) have used this reasoning to propose that Ficoll self-diffusion represents an intermediate case, where Ficoll fractional occupancy has more impact on hydrodynamic interactions than tracer size, as shown by the exponents of the concentration and radius factors. We have determined an effective viscosity (η_e) by setting $\eta_e = \eta_o D_o/D_t$, where D_o/D_t has been calculated from

Eq. 11. Using this value, along with a change in water activity in the two-parameter linear regression developed in the small cosolvent studies, $K_{m(app)} = [2.6a_w + 0.18\eta - 2.7]$ nM, the calculated $K_{m(app)}$ accounts for changes in water activity, excluded volume effects, and the nonlinear viscosity effects of Ficoll addition.

At 20% Ficoll, Fig. 5 shows that the measured value of $K_{m(app)}$ is much smaller than predicted. Equation 11 has been determined at 6.9% and 7.7% Ficoll 400 and 10.4% Ficoll 70. For 5% and 10% solutions (of Ficoll 70), effective viscosity values calculated using Eq. 11 agree closely with those calculated using the Einstein relation, $\eta_e = \eta_o(1 + 2.5\phi)$ (Schultz and Solomon, 1961) and ϕ values from a Ficoll radius of 5.5 nm determined by dynamic light scattering. The extrapolation of Eq. 11 from 10% to 20% estimates that η_e increases by ~60%, but Fig. 4 and the Einstein relation suggest that diffusion remains essentially constant between 10% and 20% solutions because excluded volume, and therefore fractional occupancy, does not increase. This idea is shown as a second set of calculated $K_{m(app)}$ values in Fig. 5. Our combined results imply that diffusion in Ficoll solutions is a simple linear function of fractional occupancy, but that Ficoll solution viscosity increases in a nonlinear fashion because of to Ficoll-Ficoll interactions.

Assuming that these ideas are correct, each of the measured values of $K_{m(app)}$ in Fig. 5 is slightly larger than the second prediction from the Einstein relation. Minton (1983) has proposed that crowding increases association rate constants while leaving dissociation constants relatively unchanged. In K_m measurements, diffusion limits the rate of bimolecular association and may attenuate the effects of excluded volume that tend to raise k_{f1}. This effect would have gone undetected in the small molecule cosolvent studies because small molecules exclude comparatively little volume. The slight difference in $K_{m(app)}$ values may also be a consequence of increased effective ionic strength, as discussed below.

V_{max} interpretation

Most of the increase in the calculated values of $V_{max(app)}$ results from excluded volume effects on effective enzyme concentration, although the estimation of $V_{max(app)}$ also includes a small modification obtained from small cosolvent studies, $V_{max} = [-171 + 183a_w]$pM/min, to account for changes in water activity. Fig. 5 shows that the measured values of $V_{max(app)}$ are much lower than the predicted values, which suggests that excluded volume may slow k_{cat}. The rate-limiting step for k_{cat} on polymer substrates is product dissociation (Baldwin et al., 1995), and the small cosolvent results have shown that $V_{max(app)}$ is not limited by diffusion up to (effective) viscosities of 2.5 cP (Wenner, 1999; Wenner and Bloomfield, 1999). Baldwin et al. (1995) have also found that k_{cat} is 10- to 50-fold smaller with polymer than with oligomer substrates and proposed that *Eco*RV transfers to nonspecific DNA on polymer substrates, which slows product dissociation. More efficient transfer or slower nonspecific dissociation as enhanced by crowded solutions may slow product dissociation and k_{cat}, although slowed dissociation disagrees with Minton's 1983 proposal that crowding predominately increases association.

Ionic strength effects

Cosolvent excluded volume may also increase effective Mg^{2+} and NaCl concentrations, which would increase the measured $K_{d,ns(app)}$ and $K_{m(app)}$ values. Changes in Mg^{2+} concentration have not been considered in the discussion above because it is unclear how effectively the relatively open, highly branched structure of Ficoll would exclude these ions.

A previous study has proposed that *E. coli* may counteract crowding effects on protein-DNA interactions by increasing cytoplasmic concentrations of K^+ (Record et al., 1998a). The majority of data in the current study on *Eco*RV have been collected under conditions well characterized in vitro, and not the typical conditions found in vivo. The data show that crowding produces large offsetting increases in V_{max}, K_m, and $K_{d,ns}$, with surprisingly little effect on the net reaction velocities compared to dilute solution rates. If in vivo reactions follow similar patterns, *Eco*RV activity in the *E. coli* cytoplasm may be relatively immune to crowding effects.

This research was supported in part by National Science Foundation grants MCB 94-18053 and MCB 97-28165.

REFERENCES

Arscott, P. G., C. Ma, J. R. Wenner, and V. A. Bloomfield. 1995. DNA condensation by cobalt hexaammine(III) in alcohol-water mixtures: dielectric constant and other solvent effects. *Biopolymers.* 36:345–364.

Baldwin, G. S., I. B. Vipond, and S. E. Halford. 1995. Rapid reaction analysis of the catalytic cycle of the EcoRV restriction endonuclease. *Biochemistry.* 34:705–714.

Berg, O. G., and C. Blomberg. 1976. Association kinetics with coupled diffusional flows. Special application to the *lac* repressor-operator system. *Biophys. Chem.* 4:367–381.

Berg, O. G., and C. Blomberg. 1977. Association kinetics with coupled diffusion. An extension to coiled-chain macromolecules applied to the *lac* repressor-operator system. *Biophys. Chem.* 7:33–39.

Berg, O. G., and C. Blomberg. 1978. Association kinetics with coupled diffusion. III. Ionic-strength dependence on the *lac* repressor-operator association. *Biophys. Chem.* 8:271–280.

Berg, O. G., and M. Ehrenberg. 1982. Association kinetics with coupled three- and one-dimensional diffusion. *Biophys. Chem.* 15:41–51.

Berg, O. G., R. B. Winter, and P. H. von Hippel. 1981. Diffusion-driven mechanisms of protein translocation on nucleic acids. 1. Models and theory. *Biochemistry.* 20:6929–6948.

Carnahan, N. F., and K. E. Starling. 1969. Equation of state for nonattracting rigid spheres. *J. Chem. Phys.* 51:635–636.

Dinnbier, U., E. Limpinsel, R. Schmid, and E. P. Bakker. 1988. Transient accumulation of potassium glutamate and its replacement by trehalose during adaptation of growing cells of *Escherichia coli* K-12 to elevated sodium chloride concentrations. *Arch. Microbiol.* 150:348–357.

Erskine, S. G., G. S. Baldwin, and S. E. Halford. 1997. Rapid-reaction analysis of plasmid DNA cleavage by the EcoRV restriction endonuclease. *Biochemistry.* 36:7567–7576.

Han, J., and J. Herzfeld. 1993. Macromolecular diffusion in crowded solutions. *Biophys. J.* 65:1155–1161.

Hou, L., F. Lanni, and K. Luby-Phelps. 1990. Tracer diffusion in F-actin and Ficoll mixtures. Toward a model for cytoplasm. *Biophys. J.* 58: 31–43.

Jeltsch, A., and A. Pingoud. 1998. Kinetic characterization of linear diffusion of the restriction endonuclease EcoRV on DNA. *Biochemistry.* 37:2160–2169.

Kellenberger, E., E. Carlemalm, J. Sechaud, A. Ryter, and G. de Haller. 1986. Considerations on the condensation and the degree of compactness in non-eukaryotic DNA-containing plasmas. *In* Bacterial Chromatin: Proceedings of the Symposium "Selected Topics on Chromatin Structure and Function," University of Camerino, Camerino, Italy, May, 1985. C. O. Gualerzi and C. L. Pon, editors. Springer-Verlag, Berlin and New York. 11–25.

Kuzmic, P. 1996. Program DYNAFIT for the analysis of enzyme kinetic data: application to HIV proteinase. *Anal. Biochem.* 237:260–273.

Lindner, R. A., and G. B. Ralston. 1997. Macromolecular crowding—effects on actin polymerisation. *Biophys. Chem.* 66:57–66.

Minton, A. P. 1981. Excluded volume as a determinant of macromolecular structure and reactivity. *Biopolymers.* 20:2093–2120.

Minton, A. P. 1983. The effect of volume occupancy upon the thermodynamic activity of proteins: some biochemical consequences. *Mol. Cell. Biochem.* 55:119–140.

Minton, A. P. 1997. Influence of excluded volume upon macromolecular structure and associations in "crowded" media. *Curr. Opin. Biotechnol.* 8:65–69.

Poon, J., M. Bailey, D. J. Winzor, B. E. Davidson, and W. H. Sawyer. 1997. Effects of molecular crowding on the interaction between DNA and the *Escherichia coli* regulatory protein TyrR. *Biophys. J.* 73: 3257–3264.

Record, M. T., E. S. Courtenay, D. S. Cayley, and H. J. Guttman. 1998a. Biophysical compensation mechanisms buffering *E. coli* protein-nucleic acid interactions against changing environments. *Trends Biochem. Sci.* 23:190–194.

Record, M. T., E. S. Courtenay, D. S. Cayley, and H. J. Guttman. 1998b. Responses of *E. coli* to osmotic stress: large changes in amounts of cytoplasmic solutes and water. *Trends Biochem. Sci.* 23:143–148.

Riggs, A. D., S. Bourgeois, and M. Cohn. 1970. The lac repressor-operator interaction. 3. Kinetic studies. *J. Mol. Biol.* 53:401–417.

Schultz, S. G., and A. K. Solomon. 1961. Determination of the effective hydrodynamic radii of small molecules by viscometry. *J. Gen. Physiol.* 44:1189–1199.

Tanford, C. 1961. Physical Chemistry of Macromolecules. John Wiley and Sons, New York.

Taylor, J. D., and S. E. Halford. 1989. Discrimination between DNA sequences by the EcoRV restriction endonuclease. *Biochemistry.* 28: 6198–6207.

Wenner, J. R. 1999. Solution effects on DNA conformation and EcoRV kinetics. Ph.D. thesis, University of Minnesota, Twin Cities.

Wenner, J. R., and V. A. Bloomfield. 1999. Osmotic pressure effects on EcoRV cleavage and binding. *J. Biomol. Struct. Dynam.* (in press).

Winkler, F. K., D. W. Banner, C. Oefner, D. Tsernoglou, R. S. Brown, S. P. Heathman, R. K. Bryan, P. D. Martin, K. Petratos, and K. S. Wilson. 1993. The crystal structure of EcoRV endonuclease and of its complexes with cognate and non-cognate DNA fragments. *EMBO J.* 12:1781–1795.

Zimmerman, S. B. 1993. Macromolecular crowding effects on macromolecular interactions: some implications for genome structure and function. *Biochim. Biophys. Acta Gene Struct. Expression.* 1216:175–185.

Zimmerman, S. B., and A. P. Minton. 1993. Macromolecular crowding: biochemical, biophysical, and physiological consequences. *Annu. Rev. Biophys. Biomol. Struct.* 22:27–65.